Proceedings of the 9th U.S. National and 10th Canadian Conference on Earthquake Engineering
Compte Rendu de la 9ième Conférence Nationale Américaine et
10ième Conférence Canadienne de Génie Parasismique
July 25-29, 2010, Toronto, Ontario, Canada • Paper No 654

SEISMIC BEHAVIOUR OF SMA REINFORCED CONCRETE BEAMS

A. Abdulridha[1], D. Palermo[2], and S. Foo[3]

ABSTRACT

Shape Memory Alloys (SMAs) are emerging as an alternative reinforcement for seismic applications. Superelastic shape memory alloys have the capability to recover inelastic strains upon unloading after experiencing significant displacement ductility demands. In addition, SMAs have the ability to dissipate energy, although significantly lower than members reinforced with conventional deformed reinforcing bars, through stable hysteretic behaviour. The primary objective of this paper is to present results of an experimental program aimed at investigating the performance of reinforced concrete beams designed with superelastic SMA longitudinal reinforcement in the plastic hinge area. Numerical research will be presented and includes the development of a preliminary constitutive hysteretic model for SMA-reinforced members. The constitutive model considers the unique stress-strain characteristics of superelastic materials, including yielding and strain hardening, and strain recovery upon unloading. The material model is incorporated in a two-dimensional nonlinear finite element program applicable for reinforced concrete membrane structures. Furthermore, analyses of the reinforced concrete beams presented herein will be discussed.

Introduction

Ductile structures are designed to respond inelastically when subjected to major earthquakes. This is generally achieved by assigning plastic hinges at specific locations in a structure. The plastic hinges, in turn, are designed to yield in flexure, while preventing non-ductile modes of failure. While this ensures that the structure does not collapse and the energy of the earthquake is properly dissipated, residual deformations should be expected. For the most part, the residual deformation is a result of the accumulation of residual strains in the reinforcement as the response progresses into the inelastic range. Significant residual deformations can lead to unserviceable structures at the end of a seismic event. Furthermore, it may prevent repair and retrofitting. Recently, however, a relatively new group of alloys known as Shape Memory Alloys (SMAs) has emerged and has gained interest amongst researchers. These alloys are attractive in seismic applications, due mostly to their capability to recover inelastic

[1]Ph.D Candidate, Dept. of Civil Engineering, University of Ottawa, 161 Louis Pasteur, Ottawa, ON, Canada
[2]Assistant Professor, Dept. of Civil Engineering, University of Ottawa, 161 Louis Pasteur, Ottawa, ON, Canada
[3]Senior Engineer (Risk Management), Public Works and Government Services Canada, Gatineau, QC, Canada

displacements. This leads to re-centering after a seismic attack. Furthermore, SMAs yield under load and strain harden at large strains. In addition, SMAs have strength capacity similar to conventional deformed reinforcing bars. A main drawback of SMAs is the high initial cost; therefore, they should be used in critical regions only. Another issue is the lower capacity to dissipate energy as a result of the re-centering characteristics of the material. To a lesser extent is the larger crack widths and crack spacing that should be expected in concrete members reinforced with SMAs as a consequence of their smooth surface. However, SMAs are resilient to corrosion and larger crack widths relative to conventional deformed bars can be tolerated. Shape memory alloys are unique materials that experience crystalline phase transformations when subjected to temperature or stress changes, and they exist in two phases: Austenite and Martensite. In the Austenite phase, the material is superelastic and is capable of recovering inelastic strains upon removal of load; whereas, the Martensite phase requires heat to recover strains. Nickel-titanium alloy is the most common type of SMA, consisting of approximately 56% nickel and 44% titanium. Fig. 1 provides a general stress-strain response of superelastic SMAs for one loading cycle. At low strains, the SMA response is linear elastic. Beyond the initial elastic region, the response substantially softens demonstrating nonlinearity followed by a near constant stress plateau. This is the result of stress-induced transformation from Austenite to Martensite and is known as forward transformation. At large strains, the material strain hardens due to the response of the stress-induced Martensite state. The initial unloading response is linear followed by a sharp recovery of strain at almost constant stress. The latter characterizes the behaviour of the material during the reverse transformation from Martensite back to Austenite. Finally, in the Austenite phase, the SMA returns to its original undeformed shape at zero stress.

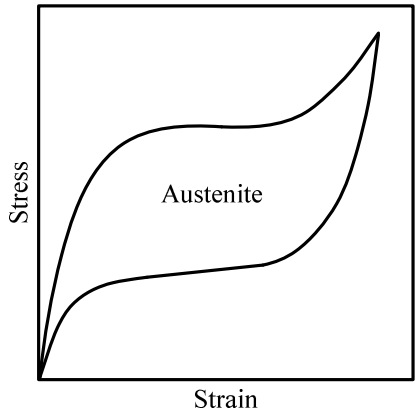

Figure 1. Typical superelastic SMA stress–strain response

A number of studies have focused on material characterization and mechanical properties of superelastic NiTi bars and wires to evaluate the material for use in structural and seismic applications (DesRoches et al. 2004; Tyber et al. 2007; McCormick et al. 2007). Specifically, McCormick et al. (2007) studied the deformation behavior of large diameter superelastic bars applicable for structural applications. The work demonstrated that the re-centering capability and equivalent viscous damping increased with a decrease in bar size. In general, full-scale large diameter bars demonstrated good pseudoelastic properties. Furthermore, loading rates were investigated and full-scale tests subjected to earthquake-type loading showed similar behavior to cyclic tests, further demonstrating the applicability of SMA bars in structural applications. A limited number of experimental studies have been conducted with superelastic SMA bars as

reinforcement for seismic applications. This includes exploratory studies on small-scale beams reinforced with either embedded or externally fastened SMAs (Saiidi et al. 2007; Deng et al. 2006). Saiidi et al. (2006; 2009) investigated the seismic behaviour of columns reinforced with SMA bars and engineered cementitious concrete in the plastic hinge region as a technique to reduce damage. Other studies have included the use of SMA embedded bars in beam-columns (Youssef et al. 2008), and SMA bars as external structural bracing elements in low-rise shear walls (Effendy et al. 2006). The focus of this paper is to highlight the potential benefits of superelastic SMA bars for seismic design of concrete structures. Experimental results of beams under reverse cyclic loading will be presented, and includes crack widths and spacing, residual crack widths, hysteretic response, energy dissipation capacity, and inelastic displacement recovery capacity. Finite element analysis will be discussed and includes a preliminary constitutive model for SMA bars.

Experimental Program

A comprehensive experimental program was conducted on 7 simply supported concrete beams tested under monotonic, cyclic, and reverse cyclic loading. The objective of this study was to assess the structural behaviour of SMA reinforced beams and to evaluate its potential as an alternative reinforcement for seismic applications. Two beams tests will be discussed in detail, Beams B3-SR and B6-NR. The former was reinforced longitudinally with conventional 10M deformed bars at the top and bottom. The latter was reinforced with 12.5 mm diameter superelastic SMA smooth bars at the critical section only. Both beams were subjected to reverse cyclic loading. The beams were 2400 mm from centre to centre of the supports, 125 mm wide and 250 mm deep. Loading was applied by two central point loads, approximately spaced at 125 mm, ensuring a constant flexural zone (critical section). The SMA bars were used over a length of 600 mm centered at the midspan of the beams. The SMA bars were threaded at the ends and connected by means of threaded mechanical couplers to conventional deformed 15M bars. The SMA bars were reshaped to a diameter of 9.5 mm over a 300 mm length to promote yielding at the midspan and away from the threaded sections located at the ends of the bars. The couplers were 12.6 mm in diameter and 50 mm in length. The shear reinforcement, consisting of 6.35 mm diameter closed stirrups, was spaced at 100 mm along the entire length of the beam. A concrete clear cover of 20 mm was provided throughout. Fig.2 provides a drawing of a typical test specimen mounted in the testing rig.

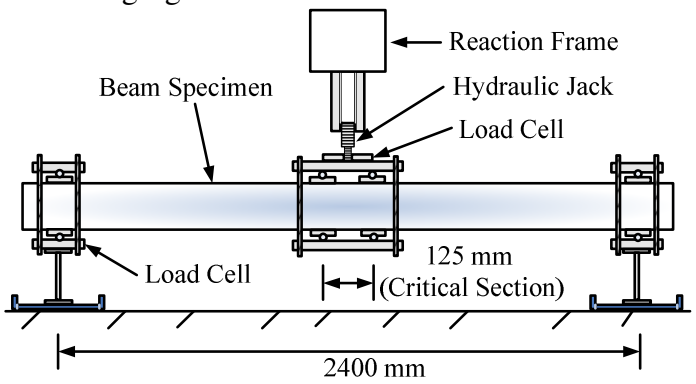

Figure 2. Typical test specimen.

Material Properties

The SMA bars used in this experimental program had a nickel to titanium ratio of 0.56:0.44 and were heat treated to produce a superelastic alloy at room temperature. Coupon samples of each reinforcement type were subjected to cyclic tensile loading to evaluate the mechanical properties. Figs. 3 a) and b) provide the response of the SMA and conventional deformed 10M bars, respectively. The modulus of elasticity of the SMA bars was approximately 60 GPa, while the modulus of elasticity of the 10M deformed bars was approximately 205 GPa. Based on a 0.2% offset, an approximate yield stress of 415 MPa was established for the SMA, slightly lower than the 425 MPa yield stress for the 10M conventional steel. The conventional steel developed strain hardening at approximately 1.5% strain. The SMA bar developed hardening at approximately 5% strain. The unloading curves of the SMA bars provide a clear differentiation between the SMA and conventional deformed bars. For the SMA bar, during the last loading cycle, the bar was strained to 7.7%, and upon unloading, the residual strain was 0.65%, representing a 91.6% strain recovery capacity. The conventional deformed 10M bar demonstrated significantly larger residual strains. During the last loading cycle to 3.54% strain, the 10M bar experienced a permanent strain of approximately 3.44%, representing a 2.8% strain recovery.

The beams were constructed with normal strength concrete. The average compressive strength on the day of testing was 32.7 MPa and 34.6 MPa, respectively for the SMA and conventional reinforced beams. The mix included a maximum aggregate size of 10 mm.

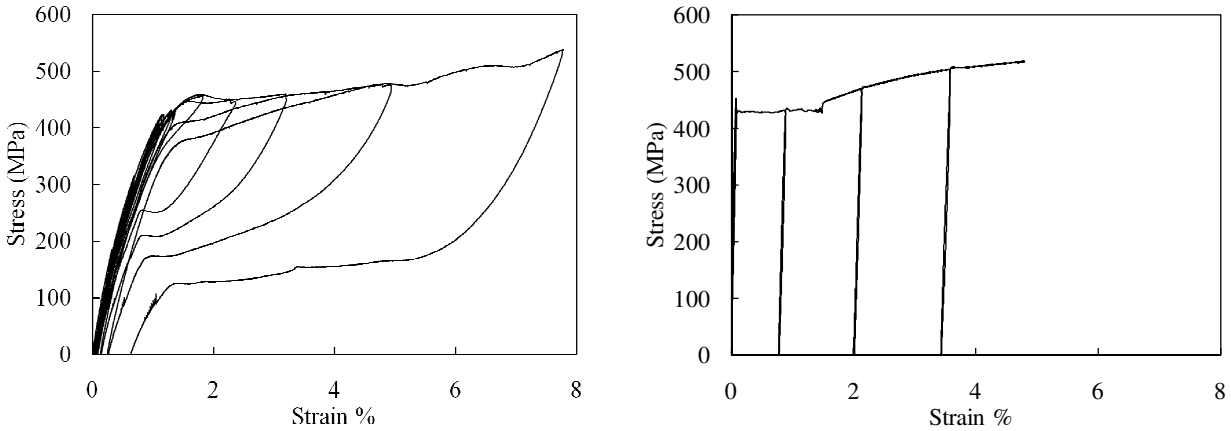

Figure 3. Stress-strain response under cyclic loading: a) SMA bar; (b) 10M deformed bar.

The specimens were tested using the testing rig illustrated in Fig. 2. A steel plate, 75 mm long, 150 mm wide, and 25 mm thick was placed under each point load to prevent crushing of the concrete. The loading was applied by a hydraulic jack using displacement control. Load cells were used to monitor the applied forces, and deflection readings were continuously recorded at the midspan using displacement cable transducers (DCTs). The reverse cyclic loading was imposed according to ATC-24 (ATC 1992), Guidelines for Cyclic Seismic Testing of Components of Steel Structures. The only modification included single repetitions at each

displacement level. The loading consisted of one cycle at 0.33Δ*y*, 0.66Δ*y*, and 1.0Δ*y*, where Δ*y* is the yield displacement. Thereafter, subsequent cycles were based on multiples of Δ*y* until failure. The yield displacement was approximately 6.4 mm and 5.7 mm, respectively, for the SMA and conventional reinforced beams.

Test Results

The load-midspan displacement responses for Beams B3-SR (steel) and B6-NR (SMA) are shown in Figs. 4 a) and b), respectively. The behaviours demonstrate that the conventional reinforced beam sustained larger load capacity and dissipated more energy; whereas, the SMA reinforced beam was capable of restoring the inelastic displacements. To assess better the capacity and ductility of each beam, the envelope normalized load-displacement ductility responses are given in Fig. 5. The responses were dominated by flexure, thus the load was normalized according to the tensile yield capacity (*Asfy*) of the reinforcement used in the critical section. Recall that the conventional reinforced beams used 10M bars (100 mm^2) with yield strength of 425 MPa, and the SMA beams used reshaped 9.5 mm diameter bars (71 mm^2) with yield strength of 415 MPa. Also, the yield displacements, according to ATC-24, were 5.7 mm and 6.4 mm, respectively, for the conventional and SMA beams. The normalized envelopes demonstrate that the responses are similar, including initial stiffness, strength capacity, yield plateau, and ultimate ductility. Therefore, SMA reinforced beams can sustain ductility and strength capacities similar to conventional reinforced beams, provided that the longitudinal reinforcement has a similar yield force capacity. The reverse cyclic responses of Fig. 4 highlight the differences, specifically the superior re-centering capability and the reduced energy dissipation capacity of the SMA beam. Both beams failed in flexure. The conventional reinforced beam experienced concrete crushing in the flexural compression zone, after significant yielding of the longitudinal reinforcement. The SMA beam also experienced concrete crushing in the flexural compression zone. In addition, the SMA ruptured at the transition zone where the bar diameter changed from 12.5 mm to 9.5 mm. This resulted in a lower than expected strength and ductility capacity.

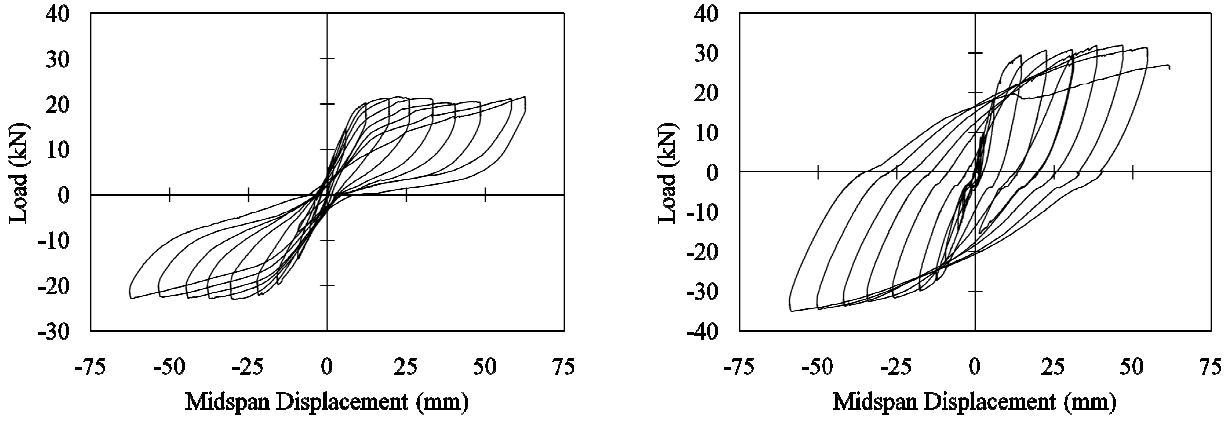

Figure 4. Load-midspan displacement response: a) SMA beam; (b) conventional beam.

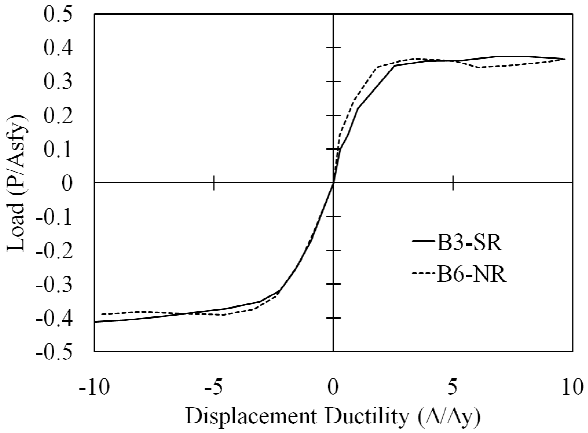

Figure 5. Envelope normalized load-displacement ductility response.

Fig. 6 illustrates the condition of the beams at the end of testing. The photos of the beams reveal a marked difference in cracking patterns. The conventional beam experienced closely spaced cracks and smaller crack widths relative to the SMA beam. The SMA bars were smooth and, therefore, lead to wider spaced cracks with larger widths. However, the SMA bars, which consist of nickel and titanium, provide resistance to corrosion similar to stainless steel. Thus, SMA bars can tolerate larger crack widths. At 6Δy, B3-SR and B6-NR experienced crack widths of 8 mm and 30 mm, respectively. Interestingly, B6-NR was capable of recovering approximately 90% of the crack opening upon removal of load, whereas B3-SR recovered only 20%.

(a) (b)

Figure 6. Failure condition: a) SMA beam (b) conventional beam.

Energy dissipation capacity is a salient feature of seismic response for structural members. Fig. 7 a) provides the normalized load-displacement ductility response at the ultimate displacement. The behaviours illustrate that the conventional reinforced beam experienced greater energy dissipation under reverse cyclic loading. The reduced energy dissipation in the SMA beam was a result of the reverse transformation during unloading, which caused pinching as the member re-centered. Furthermore, B6-NR failed by rupturing of the reinforcement at the transition zone, which resulted in reductions in strength and energy dissipation capacities.

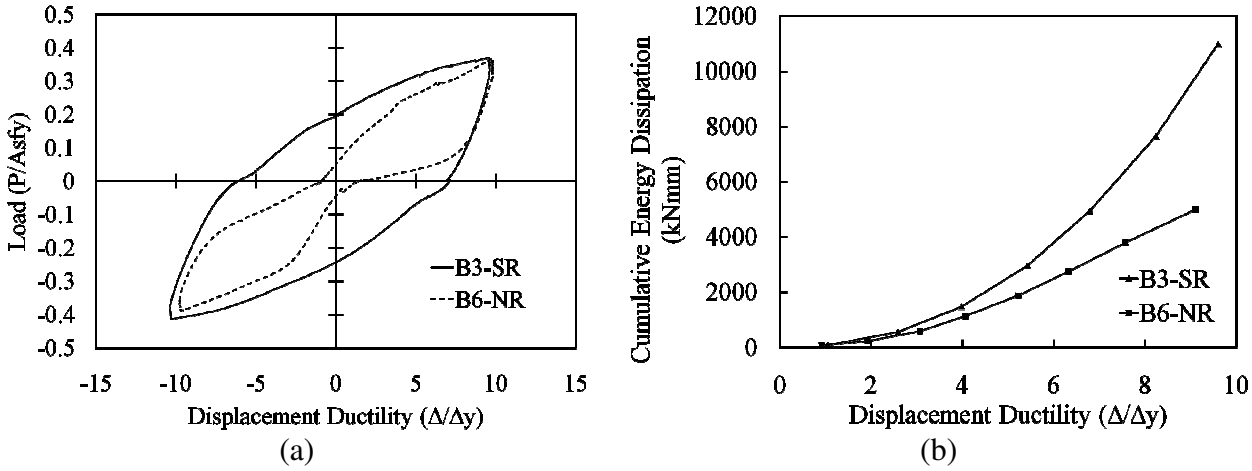

Figure 7. Energy dissipation: a) Normalized hysteretic response; b) cumulative dissipation.

Fig. 7 b) provides the cumulative energy dissipation experienced by the beams at each displacement ductility level. The energy was calculated from the area under the actual load versus midspan displacement response. The conventional reinforced beam dissipated significantly more energy than the SMA beam. At the ultimate displacement ductility, approximately 11 000 kNmm and 5 000 kNmm of energy were dissipated by the conventional and SMA reinforced beams, respectively. The response illustrates that the conventional reinforced beam dissipates energy at a great rate than the SMA reinforced beams owing to the response of the reinforcement under reverse cyclic loads. The SMA reinforced beams attempt to recenter, which causes a pinching effect and a reduction in the energy dissipation capacity. Conversely, deformed reinforcing bars accumulate permanent strains, which results in wide hysteretic curves and significant energy dissipation.

Analytical Program

The authors are involved in an ongoing analytical program, which includes development of a hysteretic constitutive model for superelastic SMA bars that considers the initial linear elastic loading curve, followed by yielding and strain hardening. In addition, consideration is given to the reloading and unloading curves such that the energy dissipation of the SMA bar is satisfactorily captured. A preliminary model has been developed and was implemented in program VecTor2 (Wong and Vecchio 2002), a nonlinear two-dimensional finite element program applicable for membrane structures. Program VecTor2 uses a smeared, rotating-crack formulation based on the Modified Compression Field Theory (1986) and the Disturbed Stress Field Model (2000). The program algorithm is based on a secant stiffness formulation using a total-load iterative procedure. The preliminary model is illustrated in Fig. 8. It includes a linear loading curve, a yield plateau and strain hardening. Unloading is assumed to be linear and fully recovers the inelastic straining. Reloading follows the unloading path and returns to the previous unloading point. Analyses were conducted on the conventional and SMA reinforced beams. The beams were modeled with rectangular plane stress elements, the transverse shear reinforcement was considered smeared within the concrete elements, and the longitudinal flexural reinforcement was modeled with truss bar elements.

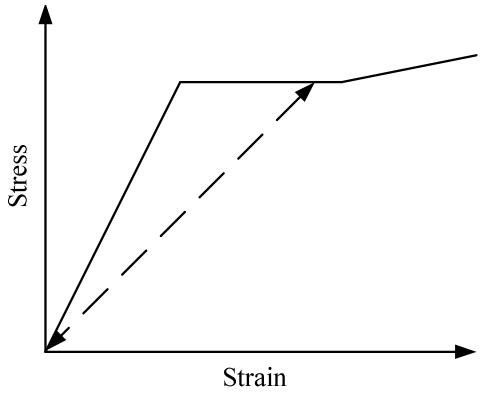

Figure 8. Preliminary SMA hysteretic model.

The model consisted of 1008 rectangular elements for the concrete and 216 truss elements for the top and bottom reinforcement. The truss bars were assumed perfectly bonded to the surrounding concrete. The loading followed the same protocol as used during testing. The default constitutive models suggested within VecTor2 were selected for the analyses. Figs. 9 a) and b) show the response of the SMA reinforced and conventional reinforced beams, respectively. In general, the strength capacities are well simulated. The response of the SMA reinforced beams indicates that the recovery is slightly overestimated and the unloading curves do not capture the nonlinear unloading response of the SMA reinforced beam observed during testing. These deficiencies are a direct result of the preliminary model that incorporates a zero plastic-offset model and assumes a linear unloading curve. For comparison purposes, the analytical response of the conventional reinforced beam is given in Fig. 9 (b). The analysis satisfactorily captured the behaviour observed during testing including strength and ductility capacities. The unloading and reloading curves were well simulated. A notable discrepancy is the pinching; slightly more was observed during testing. Improved results for the SMA beam can be achieved with a refined constitutive model for SMA bars that captures the nonlinear unloading and small residual strains accumulated as the ductility demands increase.

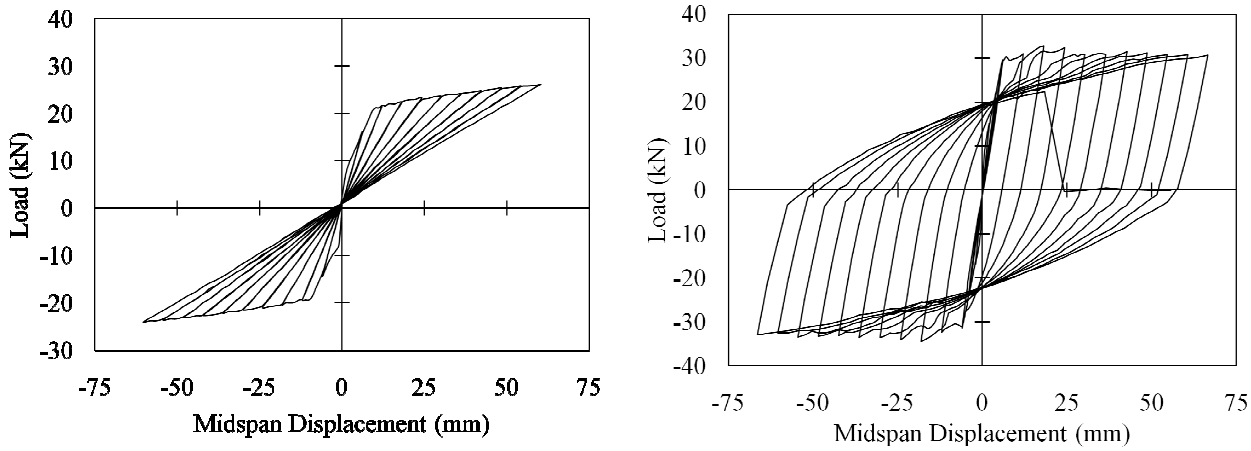

Figure 9. Analytical load-displacement response: a) SMA beam (b) conventional beam.

The numerical models were further assessed by comparing the calculated and observed cracking patterns. The model predicted closely spaced cracks in the conventional reinforced beam and significantly farther spaced cracks in the SMA reinforced beam as shown in Fig. 10. These trends were consistent with observations noted during testing, further verifying the finite element model.

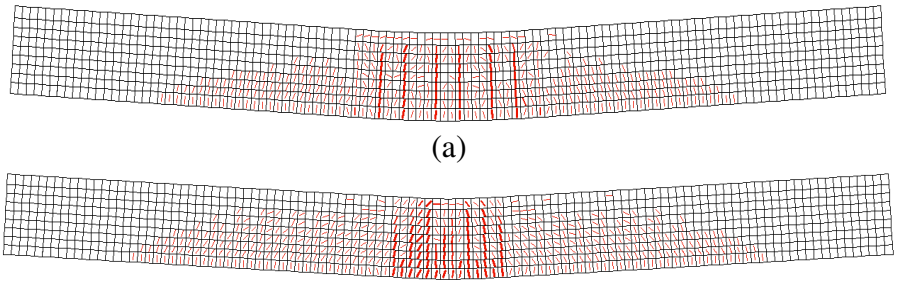

(a)

(b)

Figure 10. Predicted cracking patters: a) SMA beam (b) conventional beam.

Conclusions

The ability of shape memory alloys to recover inelastic displacements and sustain large ductility was presented in this study. In general, the experimental results demonstrated the enhanced capability of SMAs to control residual deformation when used as longitudinal reinforcement in the critical region of concrete beams. Additional conclusions include:

1. The SMA reinforced beam was superior to the conventional deformed steel reinforced beam at limiting residual displacements.
2. The SMA reinforced beam experienced similar normalized yield and ultimate loads in comparison to the conventional reinforced beam.
3. The SMA beam sustained comparable displacement ductility to the conventional reinforced beams.
4. The SMA beam dissipated significantly less energy than the conventional reinforced beam.
5. The crack widths were larger and spaced farther in the SMA reinforced beam due to the smooth bar surface. However, the SMA reinforced beam was effective at limiting the residual crack widths after removal of load.
6. Given the high initial cost of SMAs, their implementation in concrete structures should be limited to critical regions, where yielding is expected to occur.

In summary, the capacity to recover inelastic displacements, exhibit yielding and strain hardening, while sustaining large displacement ductility are structural characteristics that make superelastic SMA attractive for seismic design.

Acknowledgements

The authors wish to express their gratitude to Public Works and Government Services Canada (PWGSC) and the Canadian Seismic Research Network (CSRN) for financial assistance

on this research project.

References

ATC-24, 1992. Guidelines for Cyclic Seismic Testing of Components of Steel Structures, Applied Technology Council, Redwood City, CA.

Deng, Z., Q, Li, and H. Sun, 2006. Behaviour of concrete beam with embedded shape memory alloy wires, *Engineering Structures*, 28, 1691-1697.

DesRoches, R., McCormick, J., and Delemont, M., 2004. Cyclic properties of superelastic shape memory alloy wires and bars," *Journal of Structural Engineering,* ASCE, 130 (1), 38-46.

Effendy, E., W. I. Liao, G. Song, Y. L. Mo, and C. H. Loh, 2006. Seismic behaviour of low-rise shear walls with SMA bars, Earth & Space 2006: Engineering, Construction, and Operations in Challenging Environment, Houston, TX, 1-8.

McCormick, J., Tyber, J., DesRoches, R., Gall, K., and Maier H. J., 2007. Structural engineering with Niti II: mechanical behaviour and scaling," *Journal of Engineering Mechanics*, ASCE, 133 (9), 1019-1029.

Saiidi, M. S., M. O'Brien, and M. Sadrossadat-Zadeh, 2009. Cyclic response of concrete bridge columns using superelastic Nitinol and bendable concrete, *ACI Structural Journal*, 106 (1), 69-77.

Saiidi, M. S., M. Sadrossadat-Zadeh, C. Ayoub, and A. Itani, 2007. Pilot study of behaviour of concrete beams reinforced with shape memory alloys, *Journal of Materials in Civil Engineering*, ASCE, 19 (6), 454-461.

Saiidi, M. S., H. Wang, 2006. Exploratory study of seismic response of concrete columns with shape memory alloys reinforcement, *ACI Structural Journal*, 103 (3), 436-443.

Tyber, J., McCormick, J., Gall, K., DesRoches, R., Maier H. J., and Maksoud, A. E. A., 2007. Structural engineering with Niti I: basic materials characterization," *Journal of Engineering Mechanics*, ASCE, 133 (9), 1019-1029.

Vecchio, F. J., 2000. Disturbed stress field model for reinforced concrete: formulation, *Journal of Structural Engineering, ASCE*, 126(9), 1070-1077.

Vecchio, F.J. and M. P. Collins, 1986. The Modified compression field theory for reinforced concrete elements subject to shear, *ACI Structural Journal*, 83(2), 219-231.

Wong, P.S., and F. J., Vecchio, 2002. VecTor2 & Formworks user's manual, University of Toronto, Toronto, Canada.

Youssef, M., M. Alam, and M. Nehdi, 2008. Experimental investigation on the seismic behaviour of beam-column joints reinforced with superelastic shape memory alloys," *Journal of Earthquake Engineering*, 12, 1205-1222.